

Modeling of Corrosion Fatigue Crack Initiation under Passive Electrochemical Conditions

M.A. DAEUBLER, G.W. WARREN, I.M. BERNSTEIN, and A.W. THOMPSON

A combined mechanical/electrochemical model has been developed which successfully predicts the corrosion fatigue initiation behavior of an iron-base superalloy using readily measurable electrochemical and mechanical properties. In particular, the model uses the current decay curve, the initial or bare metal corrosion rate, and the critical slip step height, a parameter associated with the transition from an intense slip band to an incipient crack. The exponential parameter, α , used to fit the early (short time) portion of the current decay curve has been found to scale with the fatigue crack initiation time, suggesting that α could be used as a valuable screening aid to assess the corrosion fatigue susceptibility of any alloy under passive electrochemical conditions. The model permits accurate prediction of both the shape and magnitude of fatigue life ($S-N$) curves. The limitations and theoretical implications of the approach of this model are also discussed.

I. INTRODUCTION

FOR practical as well as fundamental reasons, it is of great importance to understand and predict fatigue life in terms of crack initiation and crack propagation. This research has focused on the first of these, *i.e.*, corrosion fatigue crack initiation, since this typically dominates fatigue life. Mueller^[1,2] has shown that initiation can be strongly influenced by the types of corrosion processes which occur, for example, general corrosion, localized corrosion (pitting), or passive corrosion, and has suggested a different theoretical approach to modeling in each regime. For the case of passive corrosion, initiation is believed to occur at slip steps which have penetrated the passive film^[2-7] (Figure 1).

The emergence of a slip step exposes bare metal to the environment. This metal will experience a small amount of dissolution as the passive layer is formed over the newly exposed surface. The crack initiation process may then be viewed as an interaction and competition between the rate of growth of slip steps and the rate of repassivation. Pyle and co-workers^[3,4] have, in fact, made such a correlation for a stainless steel and have measured the repassivation events by *in situ* monitoring of current transients as the material was subjected to cyclic plastic strain at a constant applied potential in the passive region. It seems reasonable that the current decay behavior, and therefore the fatigue behavior, could be significantly affected by a change in applied potential or electrolyte composition, and this has, in fact, been verified in a number of cases.^[3,4,7,8]

Clearly, the electrolyte composition in small precracks or surface cracks which results from the interaction of emerging slip steps and repassivation is also of interest. Recently, there have been a number of investigations of crack tip electrochemistry^[9-12] dealing with long through-cracks under stress corrosion cracking conditions. However, the relationship between results obtained for long cracks and small surface cracks on the order of several micrometers in depth is not clear. Turnbull and Thomas^[13] have, in fact, suggested that, other conditions being constant, the size of the crack can significantly affect the environment at the crack tip. It has been observed that for a given microstructure, crack growth rates can be less sensitive to environmental conditions than crack initiation, as is the case for alloy A-286.^[14] One possible explanation for this observation may be a difference in crack tip chemistry. This can be important, especially since changes in the aqueous environment could, in turn, significantly affect the repassivation kinetics as reflected in the current decay or current transient data.

There have been a considerable number of experimental and modeling efforts devoted to the problem of corrosion cracks and corrosion fatigue, beginning with the pioneering work of Brown^[15] and most recently expressed in several specialized conferences^[16-19] and a number of relevant papers.^[20-29] Although some of this modeling work has involved extremely complex representations of experimental data and physical parameters, we have chosen to work with a relatively simple analysis and to pursue extension and development of a partially successful model^[1,2] for the circumstance of interest, crack initiation under passive corrosion conditions.

Previous investigations^[14,30] of the corrosion and fatigue behavior of alloy A-286 in air and under passive conditions in a sulfuric acid electrolyte have provided a useful base of experimental observations for the current study. The objective of the present investigation was to develop a model for crack initiation under conditions of corrosion fatigue that would account for these experimental observations reasonably well and provide an improved understanding of the interaction between corrosion and fatigue. The model presented is based on slip step

M.A. DAEUBLER, formerly Postdoctoral Associate, Carnegie Mellon University, is with MTS-Deutsche Aerospace, Department ELMA, D-8000 Munich 50, Federal Republic of Germany. G.W. WARREN, formerly Associate Professor, Carnegie Mellon University, is Professor, Department of Metallurgical Engineering, University of Alabama, Tuscaloosa, AL 35486. I.M. BERNSTEIN, formerly Professor, Carnegie Mellon University, is Chancellor, Illinois Institute of Technology, Chicago, IL 60616. A.W. THOMPSON, Professor, is with the Department of Metallurgical Engineering and Materials Science, Carnegie Mellon University, Pittsburgh, PA 15213.

Manuscript submitted May 29, 1987.

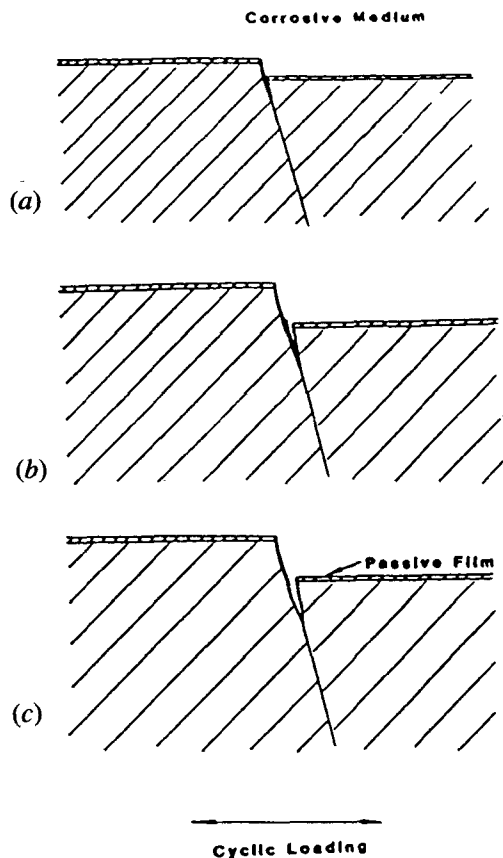


Fig. 1—Schematic illustration of slip-film rupture-repassivation model. Surface shown may be a free surface or at a crack tip. (a) Slip step ruptures surface film; bare metal begins to dissolve. (b) Penetration continues during further cycling, accompanied by greater step height if slip band remains active. (c) When process ceases, a notchlike feature remains.

dissolution and repassivation, incorporating mechanical as well as electrochemical factors, and utilizes a repeating film rupture mechanism, and as such represents an extension and refinement of the model previously proposed by Mueller.^[2] The model also attempts to relate the rate at which slip steps emerge with repassivation rates, *i.e.*, current transient measurements.

II. EXPERIMENTS

The experimental material was the iron-base superalloy, A-286, the composition, thermomechanical history, heat treatment, and microstructure of which have been described in detail previously.^[14,30] Several types of experiments were performed. Emphasis for the corrosion fatigue testing was on the underaged (denoted UA) and very underaged (VUA) microstructures.^[14,30] Fatigue tests using hourglass-shaped specimens^[14] were conducted in air and in 1M H₂SO₄ under sinusoidal loading at room temperature, using a servohydraulic testing machine and a load ratio, *R*, of 0.1. Testing frequencies were 1, 10, and 30 Hz.

Separate electrochemical experiments including potentiodynamic polarization and current decay experiments at constant potential were also performed. For these

experiments, electrodes of a known cross section were prepared from the A-286 microstructures mentioned above, mounted in epoxy, and mechanically polished through 600 grit abrasive paper immediately prior to each experiment. An initial cathodic treatment of -0.6 A for 90 seconds was also employed immediately prior to each polarization curve or current decay experiment in order to minimize the effects of any film which may have formed during exposure to air or water.^[14] All experiments were performed using either a Model 173 or 273 EG&G potentiostat, a Model 175 EG&G voltage programmer, and a Houston 2000 X-Y recorder. The 1M sulfuric acid electrolyte, with varying additions of NaCl, was used at room temperature in all experiments.

Results for the electrochemical experiments indicated that an applied potential of 0.6 V vs a saturated calomel electrode (SCE) would maintain the alloy surface in a passive state, and this value of potential was selected for the passive corrosion fatigue experiments performed in sulfuric acid.^[14] The electrochemical cell used for the fatigue experiments was constructed of an inert plastic, while the A-286 specimen surfaces were covered with an insulating stop-off lacquer, except for a 1 cm² area in the midgauge region which was the working electrode. Specimens were electrically isolated from the testing machine using ceramic inserts in the specimen grips. A Pt foil around the A-286 specimen served as the counter electrode and a saturated calomel electrode as the reference.

As in the electrochemical experiments, the fatigue specimens were subjected to a cathodic pretreatment of -0.6 A for 90 seconds immediately prior to shifting to the passive potential of 0.6 V vs SCE, which was held for 30 minutes before imposing the loading frequency. During fatigue tests, specimens were removed from the testing machine at certain intervals and examined to determine the location and extent of crack growth and to measure the height of surface slip steps using light-microscope interferometry. Additional details of the experiments are available elsewhere.^[14,30]

III. MODELING OF CORROSION FATIGUE CRACK INITIATION

As previously mentioned, the model presented here is based upon the existence of a stable passive layer on the metal surface which implies that the metal is not subjected to active dissolution except at slip steps which break through the passive film. Pitting is also neglected. It is likely that the operation of any other processes would lead to quite different mechanisms for crack initiation than the physically realistic slip step dissolution-repassivation model discussed in this paper.^[2]

The essential features of this well-discussed model involve the initial rupture or penetration of the passive layer by the emergence of a slip step, as depicted in Figure 1. The newly exposed fresh metal along such a slip step is then attacked by the surrounding corrosive medium. A dissolution-repassivation process is repetitively initiated and eventually penetrates along the slip step and into the metal matrix. The suggested resulting penetration after the first few exposure-repassivation cycles is shown schematically in Figure 1(a) by the darkened region.

Progressive penetration is anticipated to occur upon further cycling (Figure 1(b)), and a notchlike feature should eventually develop, as illustrated in Figure 1(c). The preferential penetration direction lies along the slip band due to the inherently high dislocation density and associated higher chemical activity. Such a sequence appears qualitatively reasonable. However, a complete, testable, predictive model is needed to verify such a process sequence, as detailed in the following sections.

A. The Initiation Process

A history of the proposed crack initiation process is schematically shown in Figure 2 as a plot of current density vs time, where time is equivalent to the number of cycles, N , which, in turn, is given by the product of frequency, ν , and time, t . Once the fatigue test is begun, slip steps develop but must reach a certain localized height in order to penetrate the passive film of a given thickness. The number of fatigue cycles required for penetration is given by N_0 . At this point, fresh, unprotected metal would be exposed to the corrosive environment. The corrosion current at such a slip step should increase drastically and then decay as the freshly exposed metal begins to passivate.^[2] This is shown by the first peak in Figure 2. This process will repeat each time the slip step undergoes a growth event of sufficient magnitude to expose additional unprotected matrix material. Importantly, these dissolution-repassivation events are not necessarily activated during each fatigue cycle, as has been implied in previous models.^[2] They usually require a longer time, ΔN , as discussed later. In addition, it seems certain that these intervals, ΔN , are not necessarily uniform, as has been depicted in Figure 2, a description used here only for simplicity. However, such an assumption does not affect the generality of the model, and it would still be applicable for the more mathematically complex case which includes randomly timed dissolution-repassivation events.

For each dissolution-repassivation event, a penetration depth along a slip step equivalent to the amount of metal dissolved can be calculated which is proportional to the area under the current decay curve, *i.e.*, the shaded areas in Figure 2. This is a measure of the charge passed during the repassivation process, a portion of which is attributable to dissolution. The sum of the charge passed

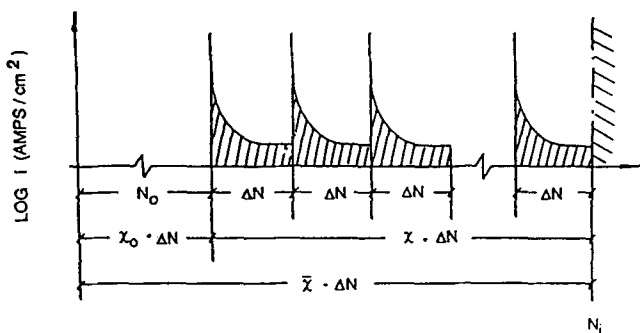


Fig. 2—Depiction of current decay history, shown as current density change over ΔN cycles, after N_0 incubation cycles (Section III-B).

for all of the dissolution-repassivation events up to the point at which the notch is equivalent to a stable crack is then proportional to a critical penetration depth, and this would define the number of fatigue cycles to crack initiation, N_i . Using the above mechanism along with a number of realistic assumptions, an equation or model for N_i has been developed.

B. Development of the Model

Since the notch (or crack) dissolution is assumed to be proportional to the total amount of charge which passes during the individual repassivation events, this charge is an important parameter to measure. Attempts to measure the current transients by an *in situ* method, such as that of Pyle and co-workers,^[3,4] were unsuccessful primarily because the applied fatigue loads were much smaller in the present work, resulting in currents which were too small to be conveniently measured. Kendig and Mansfield^[31] have recently reported a more advanced AC (alternating current) impedance technique for *in situ* monitoring of corrosion fatigue crack growth, but it has yet to be demonstrated that this technique could be applied to crack initiation. We have opted to use a more indirect technique in the present study, where current decay vs time behavior (at 0.6 V vs SCE) was determined using electrodes of A-286 mounted in epoxy. The electrodes were given the same cathodic treatment (−0.6 A for 90 seconds) as the fatigue specimens prior to imposing the passive potential. The anodic current density decay was experimentally measured, and typical results are shown in Figure 3. It was found that quite reproducible results were obtained, and the current, i , over the initial portion of the decay curve is accurately described by an equation of the following form:^{*}

$$i = i^*(kt)^\alpha \quad [1]$$

where k and α are fitting constants and the maximum current density, i^* , is defined as the measured current density at an elapsed repassivation time of 1 second. Integration of Eq. [1] then yields the amount of charge passed proportional to the amount of material dissolved during repassivation, as defined by Faraday's Law. A value of 1 second was chosen, since it was not possible to measure the current at zero elapsed time, and the response time of the X-Y recorder was approximately 1/4 to 1/3 of a second. It should be stated that this approach assumes that the effect of possible nonfaradaic processes, such as charging of the double layer or adsorption at freshly exposed metal surface areas, was either negligible or constant. According to this kind of dissolution-repassivation model, there is a direct correlation between the amount of material dissolved and the penetration depth per rupture event, d_q , as considered previously:^[2]

$$d_q = \frac{M}{zF\rho} \int_{t(q-1)}^{t(q)} i^*(kt)^\alpha dt \quad [2]$$

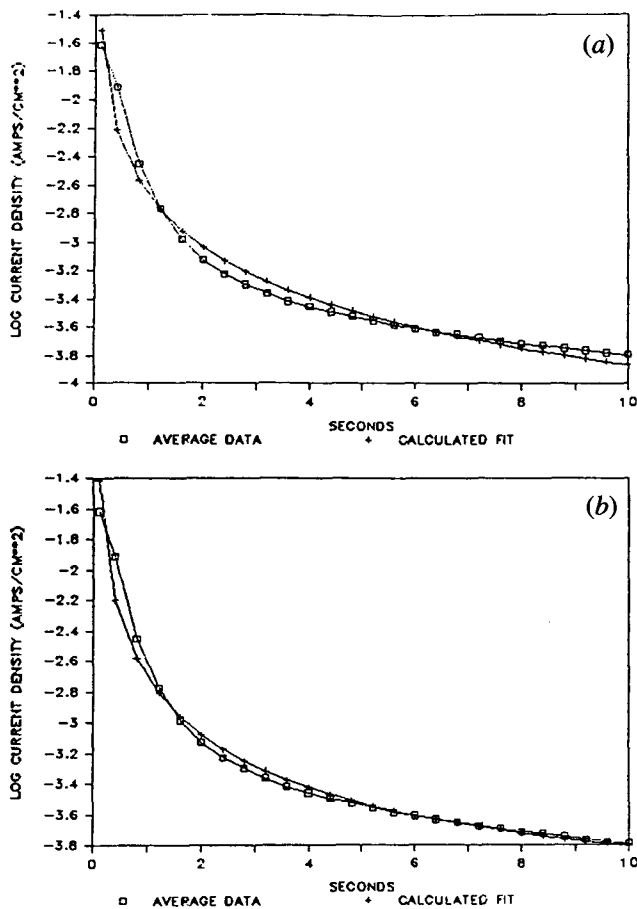


Fig. 3—Measured current decay behavior for VUA microstructure of A-286, 1 M sulfuric acid under 0.6 V vs SCE, without chloride. (a) Crosses are fitted points, using Eq. [1] with $\alpha = -0.511$. (b) Crosses are fitted with Eq. [12]; $\alpha = 0.570$ and $\beta = 0.025$.

where the preintegral term has its usual meaning. A specific number of these rupture, dissolution, repassivation events would be necessary to achieve a critical penetration depth, d_c , given by the following:

$$d_c = \sum_{q=1}^{q=X} d_q = \frac{M}{zF\rho} \sum_{q=1}^{q=X} \int_{t(q-1)}^{t(q)} i^*(kt)^\alpha dt \quad [3]$$

This approach explicitly requires that progressive local dissolution at a re-emerging slip band results in crack initiation and that preferential metal dissolution is greater at the crack tip than at its flanks. Both assumptions appear reasonable and, in fact, have been invoked extensively in previous studies.^[1,2,7] The critical penetration depth can now be related to the number of cycles required for the conversion of the notchlike feature into a defect associated with crack initiation. The following assumptions are made: constant corrosion condition and testing frequency are maintained; slip step growth events are assumed to occur intermittently with a constant time interval Δt or ΔN ; and importantly, a certain number of cycles, N_0 , are required before rupture of the passive film occurs, after which each slip step growth event is assumed to result in the same current density decay curve, as shown in Figure 2. While for a given testing fre-

quency and stress ratio, it is likely that the heights of emerging slip steps during each growth event are distributed over a range of sizes, for simplification an average (constant) slip step growth per event is taken and expressed as a multiple of the Burgers vector, nb .

Since the critical penetration depth, d_c , and the critical slip step height, SSH_c , are interdependent, the total number of growth or penetration events, $\bar{\chi}$, is estimated as follows:

$$\bar{\chi} = \frac{SSH_c}{nb} = \chi_0 + \chi \quad [4]$$

where χ is the number of slip step growth events from film rupture to initiation and χ_0 is the number of events to film rupture defined by

$$\chi_0 = \frac{h_f}{nb} \quad [5]$$

where h_f is the thickness of the passive film. With these assumptions, the integration and summation in Eq. [3] can be readily performed, yielding the following result:

$$d_c = \frac{Mi^*\chi}{zF\rho(1+\alpha)k} (k\Delta t)^{1+\alpha} \quad [6]$$

As illustrated in Figure 2, the number of cycles to crack initiation, N_i , can be expressed as

$$N_i = N_0 + \sum_{q=1}^{q=X} \Delta N_q \quad [7]$$

Since the number of cycles is also equal to the product of frequency and time, N_i can also be expressed as follows:

$$N_i = (\chi_0 + \chi)\Delta N = \bar{\chi}\Delta N = \bar{\chi}v\Delta t \quad [8]$$

Equation [6] can now be solved for Δt , and the result substituted into Eq. [8], yielding^[9]

$$N_i = \frac{\bar{\chi}v}{k} \left[\frac{zF\rho(1+\alpha)k}{Mi^*\chi} \right]^{1/(1+\alpha)} (d_c)^{1/(1+\alpha)} \quad [9]$$

This is an argument relying only on localized dissolution. To be meaningful, it should also be possible to obtain or express the critical penetration depth, d_c , from fracture mechanics. The details of such a derivation are provided in an Appendix and given here by Eq. [10]:

$$d_c = a_c \left(\frac{\sigma_a}{\sigma_f} \right)^{-2} \quad [10]$$

We can then make the important step of coupling the mechanical and electrochemical aspects of a sized defect associated with corrosion fatigue crack initiation by combining Eqs. [9] and [10]. The ensuing expression (Eq. [11]) for the number of cycles to crack initiation is thus obtained in terms of parameters which can either be reasonably estimated or experimentally measured and is therefore directly testable.

$$N_i = \frac{SSH_c v}{nbk} \left[\frac{zF\rho(1+\alpha)nbka_c}{Mi^*(SSH_c - h_f)} \right]^{1/(1+\alpha)} \left(\frac{\sigma_a}{\sigma_f} \right)^{-2/(1+\alpha)} \quad [11]$$

C. Comparison of the Model with Experimental Results

Using the data provided in Table I for the various estimated and experimentally measured parameters, the model described by Eq. [11] can be used to generate theoretical $S-N$ curves for comparison with experimental data^[14] for A-286, as well as the earlier work by Mueller.^[2] For this comparison, we and Mueller^[2] regard initiation as dominant in $S-N$ fatigue life and thus identify N_i from Eq. [11] with life. Figure 3(a) shows a typical fit to the current decay curve to obtain the exponent, α . Figure 3(b) is discussed below. Figure 4(a) shows the fit obtained by Mueller for his model, while 4(b) fits his data to Eq. [11] using the appropriate data from Table I. Only for the latter case does the predicted curve show the proper curvature. Figures 5 and 6 illustrate the excellent fit obtainable from this model for A-286 for the two heat treatments (UA and VUA) with and without the presence in solution of chloride, a depassivating agent.^[14] In all cases, the model provides excellent agreement with experiment, predicting the curvature and slope observed experimentally.

This approach allows us to predict trends in corrosion fatigue susceptibility from current decay kinetics. Figure 7 shows the relationship between the $S-N$ curve and the current decay curve. A shift in the current decay curve to lower values of current results in a lower value of the current decay exponent, α , which affects the $S-N$ curve in several ways, most noticeably an increased life prior to crack initiation. This suggests that α can be used to rank the relative susceptibility of different materials to corrosion fatigue under passive film conditions. Since it is only a fitting parameter, several alternate approaches were used to obtain a mathematical expression which might more accurately fit the experimentally measured current decay data.

A comparison of the two best fits are shown in Figures 3(a) and (b) for a single parameter and double parameter least-squares fit of the average of three separate current decay experiments at a constant applied potential of 0.6 V vs SCE. The former was obtained from Eq. [1] and the latter by Eq. [12]:

Table I. Parameters Used in Equation [11] to Obtain Predicted $S-N$ Curves

Parameter	A-286	
	Mueller's Data ^{[2]*}	(Present Study)
n	1 to 5	1 to 5
b (nm)	0.25	0.25
z (eq · mole ⁻¹)	2.0	2.0
F (A · s · eq ⁻¹)	96,500	96,500
P (g · cm ⁻³)	8.0	8.0
M (g · mole ⁻¹)	56.0	56.0
h_f (nm)	2 to 3	2 to 3
SSH_c (nm)	100	80
i^* (mA · cm ⁻²)	10(×1), 100(×5)	1 to 10**
α	-0.5(×1), -0.75(×5)	-0.4 to -0.6**

*Where the data is sensitive to alloy composition, the alloy designation is given.

**Exact value depends on the electrolyte chosen.

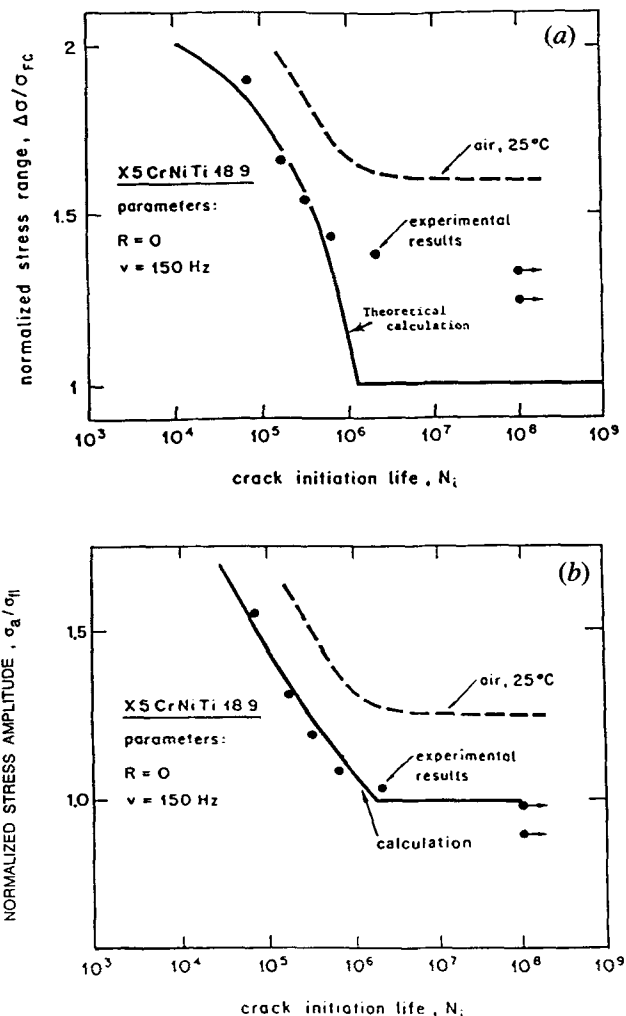


Fig. 4—Comparison of models to data by Mueller,^[2] with stress amplitude normalized by the fatigue limit in corrosion. (a) Mueller's model^[2] with his fit and (b) fit of present model (Eq. [11]) to same data.

$$i = i_1^*(kt)^\alpha + i_2^*e^{Bt} \quad [12]$$

Equations [1] and [12] fit the experimental curve quite well for very short times, as shown in Figure 3, but for times over about 1 minute, a double parameter fit (Eq. [12]) was found to be more appropriate. However, while the latter allows a slightly better fit, at longer times the calculation of the crack initiation life becomes unduly complicated, and since a significantly better prediction of the $S-N$ curve could not be obtained from Eq. [12], the single parameter fit using α was preferred. Mueller,^[2] on the other hand, used a different single parameter fit for the current decay behavior which was identical to the second term in Eq. [12]. It may be significant that both Eqs. [1] and [12] provide a much better prediction of the experimentally measured current decay behavior at very early times than does the equation used by Mueller. This would suggest that the most important contribution of the balance between dissolution and repassivation occurs at short times or high current densities, which is reasonable.

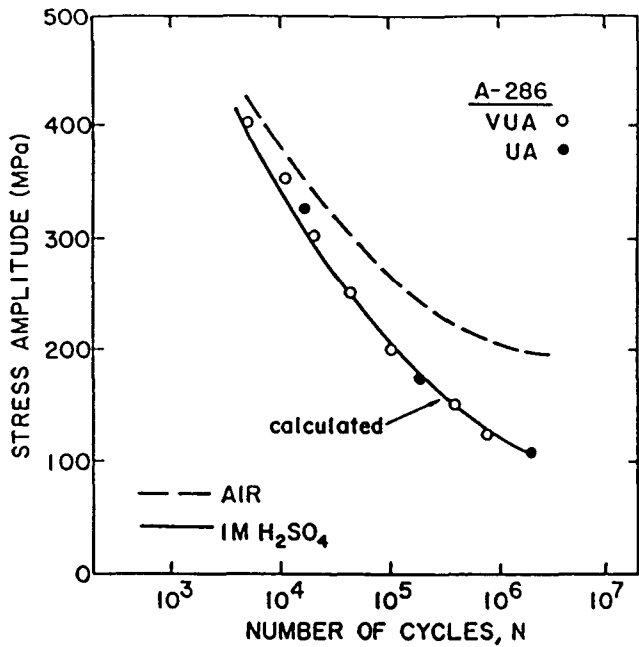


Fig. 5—Comparison of our corrosion fatigue results^[14] with the model (Eq. [11]) for VUA and UA microstructures of A-286, shown as stress amplitude (S) vs cycles to failure (N).

IV. DISCUSSION

From the comparison of data shown in Figures 4 through 6, it is obvious that the proposed model represents a significant improvement in corrosion fatigue crack initiation predictions. While the application of Eqs. [1] through [4] may be quite general, the lack of necessary detailed statistical data required some simplifying assumptions to enable a reasonable calculation of the number of cycles

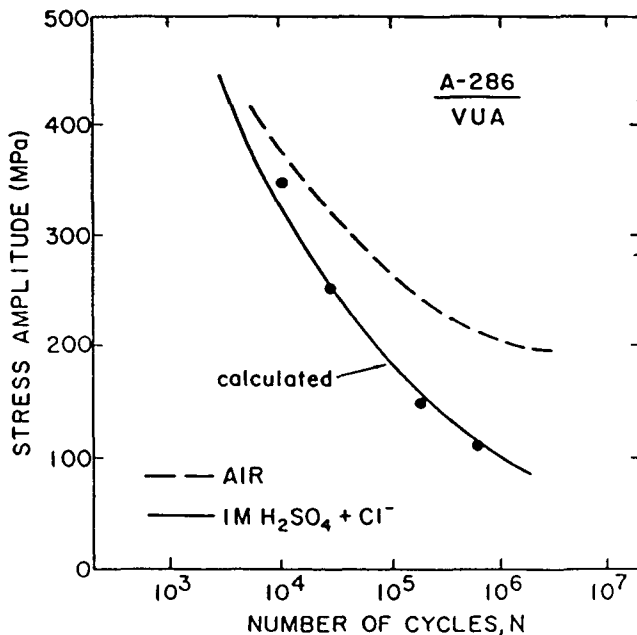


Fig. 6—Comparison of data^[14] to model, as in Fig. 5 but for 1000 ppm chloride addition to environment.

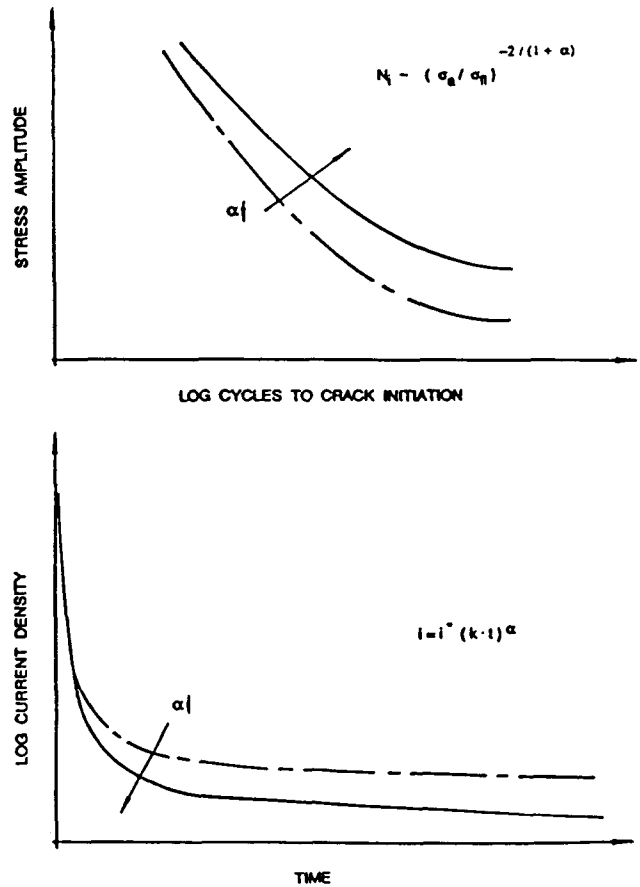


Fig. 7—Relation between S - N curve and repassivation current decay. Relevant equations shown for each curve. (Top) S - N curves, showing that decreasing α raises curve; (bottom) current decay curve, showing that decreasing α corresponds to a lower curve.

to crack initiation, N_i , as expressed by Eq. [11]. It is worthwhile to re-examine these assumptions and also to identify limitations to the model.

The term N_i is essentially a combined function of mechanical and electrochemical factors relating the passive film and its rupture not only through parameters like SSH_c and h_f but also through microstructurally sensitive terms such as σ_{fl} , a_c , and $n\mathbf{b}$. The initial corrosion current in the crack is considered to be reflected by the rate of corrosion of bare metal. However, the current at the crack tip along the slip band may, in fact, be larger due to the accumulation of dislocations at this point or to an electrolyte at the crack tip which differs from the bulk electrolyte. Neither of these factors should alter the sense or likely the magnitude of the correlation between the current at the crack tip and the bare metal corrosion current. Both i^* and α are expected to be dependent on electrolyte composition (e.g., Cl^- , pH, etc.) and applied potential, as would be the passive film thickness, h_f . The connection between electrochemistry and mechanics resides mainly in the interdependencies of the critical slip step height, SSH_c , and h_f .

Thus, the model provides a generalized parametric description of fatigue crack initiation, which, for a given set of material, electrochemical conditions, and testing parameters, would predict that corrosion fatigue crack

initiation is a function only of the applied stress amplitude, σ_a . For purposes of examining whether such a prediction is an undue simplification, the variables n , i^* , and α have been calculated by determining the best fit of Eq. [11] to the experimentally measured $S-N$ curve. Values obtained are: $n = 1$ to 5, $i^* \sim 1$ to 10 mA/cm², and $\alpha \sim 0.4$ to -0.6 . While these are reasonably close to values that were assumed or experimentally measured, such correlative support should not be over-emphasized. In fact, a number of problems with the approach persist.

In the derivation of Eq. [11], the assumption was made that the slip step growth increment can be expressed as an integral number of Burgers vectors, $n\mathbf{b}$, for a particular testing frequency, implying that the statistical distribution of slip step growth increments is expected to be a function of test frequency. If this is the case, N_i is not linearly dependent on frequency, as Eq. [11] would suggest, but is likely a more complex function of both frequency, ν , and slip step growth increment, $n\mathbf{b}$. In fact, tests run over a range of frequencies (Figure 8) demonstrate that a linear dependence of N_i on ν does not exist. We can attempt to account for this by assuming that the slip step height growth, $n\mathbf{b}$, is a direct function of ν . For example, at the same applied stress amplitude, plastic deformation in terms of $n\mathbf{b}$ is assumed higher at 1 Hz than at 10 Hz. From Eq. [11], assuming a value of -0.5 for α , the number of cycles to crack initiation can be expressed as

$$N_i \propto \nu n\mathbf{b}$$

If average numbers of 2 and 4 are assumed for n at 10 and 1 Hz, respectively, then values of $20\mathbf{b}$ and $4\mathbf{b}$ are obtained for the product $\nu n\mathbf{b}$. This would indicate that a tenfold increase in frequency would affect the number of cycles to crack initiation only by a factor of 5, close to that observed experimentally in Figure 8. Neverthe-

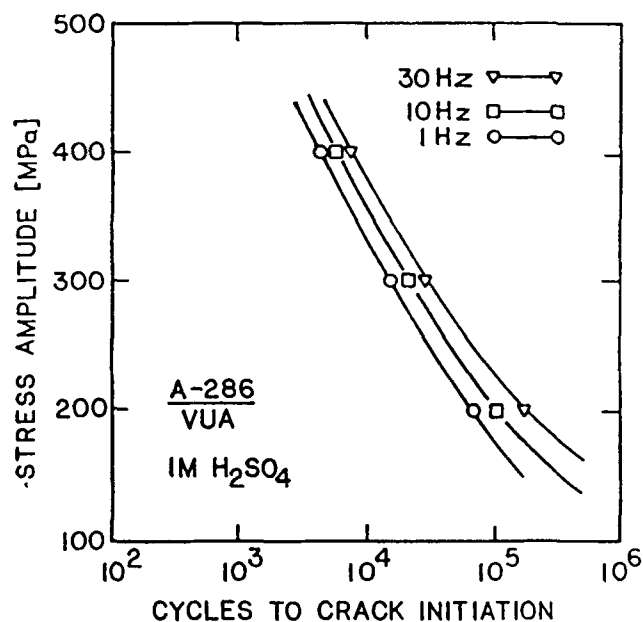


Fig. 8—Effect of cyclic frequency on $S-N$ curves for VUA microstructure of A-286.

less, by utilizing average values of the appropriate parameters, crack initiation predictions are in surprisingly good agreement and well within typical scatter for experimentally measured values^[14] of N_i .

The present model, as expressed by Eq. [11], contains a large number of parameters. Most, however, represent quantities which can be measured independently. Characterization of the current decay curves, by Eq. [1] or [12], is the most problematical part of the model, although experimental observations constrain significantly the flexibility of the corresponding parameters. As has been made clear in prior work on modeling corrosion fatigue,^[1,2,5-7,15-29,32-38] a phenomenon as complex as this inevitably requires a complex model. We have conducted a rough sensitivity analysis for the present model by experimenting with variations in all of the parameters in Eq. [12] in a computer representation of the model. Most of the variables permit only minor shifts in magnitude before the fits in Figures 4(b), 5, and 6 lose the experimental shape, magnitude, or both. Accordingly, we conclude that Eq. [11] is not only physically and mathematically reasonable but is also a fairly stringent combination of variables, albeit a complex one. Additional work on the underlying physical behavior, particularly the current decay phenomena accompanying repassivation, would be helpful and welcome.

V. CONCLUSIONS

A model for corrosion fatigue crack initiation under passive electrochemical conditions has been developed by refining and extending one previously proposed by Mueller.^[2] The present model has attempted to incorporate more realistic physical assumptions for both electrochemical and metallurgical parameters and has for the first time explicitly included actual experimental measurement of the current decay curve, initial or bare metal corrosion rate, and critical slip step height in predictive relations. Measurement of slip step height development made clear that a slip step does not grow during each fatigue cycle but indicated that growth must instead be intermittent and must occur in multiples of the Burgers vector of order 1 to 5. By mathematically fitting the experimental current vs time data, the value of the exponent α obtained is in good agreement with that calculated directly from experimental $S-N$ data, as is the value of the initial current density, i^* . This strongly suggests that a determination of the current decay exponent, α , from the initial portion of the current vs time data is in and of itself quite sufficient to accurately model the experimental $S-N$ data. Thus, it is the initial few seconds of the current transient that are important in the repassivation events at emerging slip steps. Since this was not appreciated in the previous model proposed by Mueller,^[2] it may explain why that model was unable to predict the appropriate curvature of the $S-N$ curve.

If further studies on other materials under passive film conditions indeed confirm that the form of the early portion of the repassivation current on a bare metal surface, reflected in α , can provide a ranking of relative susceptibility to corrosion fatigue, then the value of this present work will go well beyond the development of a successful predictive model.

GLOSSARY

i	current density, $A \cdot cm^{-2}$
i^*	potentiostatic current density at an elapsed time of 1 s, $A \cdot cm^{-2}$
k	dimension factor, s^{-1}
SSH_c	critical slip step height, nm
h_f	passive film thickness, nm
b	Burgers vector, nm
n	number of Burgers vector
z	number of electrons involved in the dissolution process, $eq \cdot mol^{-1}$
F	Faraday's constant, $A \cdot s \cdot eq^{-1}$
M	atomic weight, $g \cdot mole^{-1}$
a_c	critical intrinsic crack length at the fatigue limit, cm
R	ratio of the minimum stress, σ_{min} , to the maximum stress, σ_{max}
d_c	critical penetration depth
d_q	penetration depth per rupture event
N	number of cycles
N_i	number of cycles to crack initiation
N_0	number of fatigue cycles required for rupture of the passive film
N_q	number of cycles per rupture event
α, β	current density decay exponents
ρ	density of the material, $g \cdot cm^{-3}$
χ_0	number of slip step growth events to film rupture
χ	number of slip step growth events from film rupture to crack initiation
$\bar{\chi}$	total number of slip step growth events to crack initiation
ν	testing frequency, s^{-1}
σ_a	applied stress amplitude, MPa
σ_{min} , σ_{max}	minimum and maximum applied stress amplitude, respectively
σ_f	fatigue limit, MPa

APPENDIX

According to Tanaka and co-workers,^[9,10] the growth threshold of small fatigue cracks generally can be described using the conventional ΔK concept:

$$\Delta K = \Delta\sigma(\pi a)^{1/2} \cdot C \quad [1A]$$

with $\Delta\sigma$ is the applied stress range, a is the crack depth, and C is the configuration correction factor. The threshold stress intensity can be expressed by a combination of stress amplitudes and crack lengths. However, in a $\log \Delta\sigma$ - $\log a$ plot, ΔK_{th} represents a straight line with a slope of $-1/2$, as pictured in Figure A1. Additionally, a horizontal line can be drawn representing the fatigue strength or (as appropriate) the fatigue limit, σ_f . From the intersection of both lines, ΔK_{th} is defined by σ_f and the critical crack depth, a_c . For fatigue specimens with crack initiation occurring within a surface grain, one half of the grain size is a good approximation for a_c .^[9,10] We have discussed the Tanaka analysis and related issues elsewhere.^[39,40]

Knowing σ_f and estimating $a_c \approx d/2$, ΔK_{th} at the fatigue strength or limit can be calculated for a given configuration correction factor C :

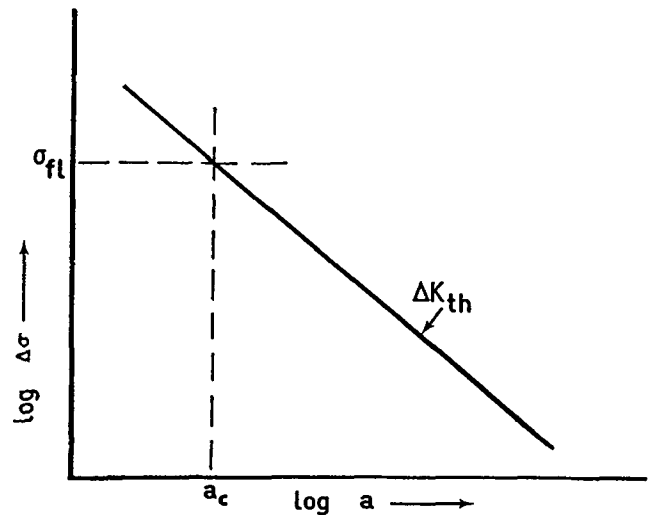


Fig. A1—Identification of parameters a_c and σ_f from plot of ΔK_{th} in $\log \Delta\sigma$ - $\log a$ space.

$$\Delta K_{th} = 2\sigma_f \left(\pi \frac{d}{2} \right)^{1/2} \cdot C \quad [2A]$$

Any critical crack depth can now be calculated as a function of applied stress by introducing Eq. [2A] (for the fatigue limit) in Eq. [1A] (general function), resulting in

$$d_c \equiv a = a_c \left(\frac{\sigma_a}{\sigma_f} \right)^{-2} \approx \frac{d}{2} \left(\frac{\sigma_a}{\sigma_f} \right)^{-2} \quad [3A]$$

The applicability of this analysis might be limited if major differences in occluded crack chemistry occur as a function of crack length.^[13,22,27] In such cases, a crack length dependence could be added to the present model.

ACKNOWLEDGMENTS

The authors would like to acknowledge the financial support provided by Contract No. DE-Fgo2-84ER45149 from the Office of Basic Energy Sciences of the United States Department of Energy. The authors also wish to express their appreciation to Mr. D.M. Solomon for helpful and insightful computations and discussions and to Mr. A. Tanzer for experimental assistance.

REFERENCES

1. M. Mueller: *Corrosion*, 1982, vol. 38, pp. 431-36.
2. M. Mueller: *Metall. Trans. A*, 1982, vol. 13A, pp. 649-55.
3. T. Pyle, V. Rollins, and D. Howard: *J. Electrochem. Soc.*, 1975, vol. 122, pp. 1445-53.
4. C. Patel, T. Pyle, and V. Rollins: *Met. Sci.*, 1977, vol. 11, pp. 185-95.
5. C. Laird and J. Duquette: in *Corrosion Fatigue* (NACE-2), O. Devereux, A.J. McEvily, and R.W. Staehle, eds., NACE, Houston, TX, 1972, pp. 88-115.
6. J.C. Scully: in *Environment-Sensitive Fracture of Engineering Materials*, Z.A. Foroulis, ed., TMS-AIME, Warrendale, PA, 1979, pp. 71-90.
7. T. Nakayama and M. Takano: *Corrosion*, 1986, vol. 42, pp. 10-15.
8. J.W. Martin and D.E. Talbot: *Nucl. Technol.*, 1981, vol. 55, pp. 499-504.
9. K. Tanaka, Y. Nakai, and M. Yamashita: *Int. J. Fract.*, 1981, vol. 17, pp. 519-33.

10. K. Tanaka and Y. Nakai: in *Fatigue Crack Growth Threshold Concepts*, D.L. Davidson and S. Suresh, eds., TMS-AIME, Warrendale, PA, 1984, pp. 497-516.
11. R. Summitt: Final Report No. N00014-K-0419, Michigan State University, East Lansing, MI, March 1986.
12. T.W. Crooker and J.A. Hauser II: NRL Memorandum Report 5763, Naval Research Laboratory, Washington, DC, April 1986.
13. A. Turnbull and J.G.N. Thomas: *J. Electrochem. Soc.*, 1982, vol. 129, pp. 1412-22.
14. M.A. Daeubler, A.W. Thompson, and I.M. Bernstein: *Metall. Trans. A*, 1991, vol. 22A, pp. 513-19.
15. B.F. Brown: in *Stress Corrosion Cracking and Hydrogen Embrittlement of Iron Base Alloys*, J. Hochmann, J. Slater, R.D. McCright, and R.W. Staehle, eds., NACE, Houston, 1976, pp. 747-50.
16. *Corrosion Fatigue—Mechanics, Metallurgy, Electrochemistry and Engineering*, STP 801, T.W. Crooker and B.N. Leis, eds., ASTM, Philadelphia, PA, 1983.
17. *Embrittlement by the Localized Crack Environment*, R.P. Gangloff, ed., TMS-AIME, Warrendale, PA, 1984.
18. *Modeling Environmental Effects on Crack Growth Processes*, R.H. Jones and W.W. Gerberich, eds., TMS-AIME, Warrendale, PA, 1986.
19. *Small Fatigue Cracks*, R.O. Ritchie and J. Lankford, eds., TMS-AIME, Warrendale, PA, 1986.
20. R.P. Wei and G.W. Simmons: *Int. J. Fract.*, 1981, vol. 17, pp. 235-47.
21. K. Landes, J. Congleton, and R.N. Parkins: in *Embrittlement by the Localized Crack Environment*, R.P. Gangloff, ed., TMS-AIME, Warrendale, PA, 1984, pp. 59-74.
22. R.P. Gangloff: *Metall. Trans. A*, 1985, vol. 16A, pp. 953-69.
23. A. Turnbull and D.H. Ferriss: in *Modeling Environmental Effects on Crack Growth Processes*, R.H. Jones and W.W. Gerberich, eds., TMS-AIME, Warrendale, PA, 1986, pp. 3-39.
24. R.H. Jones, M.J. Danielson, and C.A. Oster: in *Modeling Environmental Effects on Crack Growth Processes*, R.H. Jones and W.W. Gerberich, eds., TMS-AIME, Warrendale, PA, 1986, pp. 41-54.
25. B.N. Leis: in *Modeling Environmental Effects on Crack Growth Processes*, R.H. Jones and W.W. Gerberich, eds., TMS-AIME, Warrendale, PA, 1986, pp. 301-19.
26. R.A. Cottis: in *Small Fatigue Cracks*, R.O. Ritchie and J. Lankford, eds., TMS-AIME, Warrendale, PA, 1986, pp. 265-68.
27. A. Turnbull and R.C. Newman: in *Small Fatigue Cracks*, R.O. Ritchie and J. Lankford, eds., TMS-AIME, Warrendale, PA, 1986, pp. 269-88.
28. F.P. Ford and S.J. Hudak: in *Small Fatigue Cracks*, R.O. Ritchie and J. Lankford, eds., TMS-AIME, Warrendale, PA, 1986, pp. 289-308.
29. M. Barbosa: *Corrosion*, 1987, vol. 43, pp. 309-18.
30. M.A. Daeubler, A.W. Thompson, and I.M. Bernstein: *Metall. Trans. A*, 1988, vol. 19A, pp. 301-08.
31. M. Kendig and F. Mansfield: *Application of Electrochemical and Mechanical Impedance Techniques for Evaluation of Stress Corrosion Cracking and Corrosion Fatigue*, Proc. Corrosion Research Symp., NACE, Houston, TX, 1986, in press.
32. H.H. Johnson and P.C. Paris: *Eng. Fract. Mech.*, 1970, vol. 1, pp. 3-45.
33. R.P. Wei: *Eng. Fract. Mech.*, 1970, vol. 1, pp. 633-51.
34. R.W. Staehle: in *The Theory of Stress Corrosion Cracking of Alloys*, J.C. Scully, ed., NATO, Brussels, Belgium, 1971, pp. 223-86.
35. A. Boateng, J.A. Begley, and R.W. Staehle: *Corrosion*, 1980, vol. 36, pp. 633-38.
36. D.J. Duquette: in *Environment-Sensitive Fracture of Engineering Materials*, Z.A. Foroulis, ed., TMS-AIME, Warrendale, PA, 1979, pp. 521-37.
37. G.T. Burstein and P.I. Marshall: *Corros. Sci.*, 1984, vol. 24, pp. 449-62.
38. A. Turnbull and D.H. Ferriss: *Corros. Sci.*, 1986, vol. 26, pp. 601-28.
39. G.T. Gray, A.W. Thompson, and J.C. Williams: *Metall. Trans. A*, 1985, vol. 16A, pp. 753-60.
40. M.A. Daeubler, A.W. Thompson, and I.M. Bernstein: *Metall. Trans. A*, 1990, vol. 21A, pp. 925-33.